AGU ADVANCING EARTH AND SPACE SCIENCES

Water Resources Research

RESEARCH ARTICLE
10.1029/2023WR035617

Extending Active Network Length Versus Catchment Discharge Relations to Temporarily Dry Outlets

Gianluca Botter[1], **James McNamara**[2], **and Nicola Durighetto**[1]

[1]Department of Civil, Environmental and Architectural Engineering, University of Padua, Padua, Italy, [2]Department of Geoscience, Boise State University, Boise, ID, USA

Key Points:

- Active network length (L) versus catchment discharge (Qsur) relations are extended to temporarily dry outlets
- All the L(Qsur) relations represent translations/truncations of the spatial cumulative distribution of the specific subsurface capacity
- The L(Q_{sur}) law is not fully visible if the outlet is less persistent than other network nodes (as in a spring-fed stream drying upward)

Supporting Information:

Supporting Information may be found in the online version of this article.

Correspondence to:

G. Botter,
gianluca.botter@dicea.unipd.it

Citation:

Botter, G., McNamara, J., & Durighetto, N. (2024). Extending active network length versus catchment discharge relations to temporarily dry outlets. *Water Resources Research*, *60*, e2023WR035617. https://doi.org/10.1029/2023WR035617

Received 19 JUN 2023
Accepted 30 NOV 2023

Author Contributions:

Conceptualization: Gianluca Botter, James McNamara, Nicola Durighetto
Data curation: Nicola Durighetto
Formal analysis: Gianluca Botter, Nicola Durighetto
Funding acquisition: Gianluca Botter
Investigation: Gianluca Botter
Methodology: Gianluca Botter, Nicola Durighetto
Project Administration: Gianluca Botter
Software: Nicola Durighetto
Visualization: Nicola Durighetto
Writing – original draft: Gianluca Botter

Abstract River networks are not steady blue lines drawn in a map, since they continuously change their shape and extent in response to climatic drivers. Therefore, the flowing length of rivers (L) and the corresponding catchment-scale streamflow (Q_{sur}) co-evolve dynamically. This paper analyzes the relationship between the wet channel length and the streamflow of a river basin, formulating a general analytical model that includes the case of temporarily dry outlets. In particular, the framework relaxes the common assumption that when the discharge at the outlet tends to zero the upstream flowing length approaches zero. Different analytical expressions for the $L(Q_{sur})$ law are derived for the cases of (a) a perennial outlet; (b) a non-perennial outlet that dries out only when the whole network is dry; and (c) a temporarily dry outlet, that experiences surface flow for less time than other network nodes. In all cases, the shape of the $L(Q_{sur})$ relationship is controlled by the distribution of the specific subsurface discharge capacity along the network. For temporarily dry outlets, however, the relation between L and Q_{sur} might depend on an unknown shifting factor. Three real-world examples are presented to demonstrate the flexibility and the robustness of the theory. Our results indicate that the whole shape of the $L(Q_{sur})$ relation might not be empirically observable if a significant fraction of the network is perennial or some reaches in the network experience surface flow for longer than the discharge gauging station. The study provides a basis for integrating empirical $L(Q_{sur})$ data gathered in diverse sites.

1. Introduction

River networks continuously change their total flowing length—and the spatial configuration of wet channels—in response to time-variable hydrologic conditions in the surrounding landscape (Datry et al., 2014; Messager et al., 2021; Skoulikidis et al., 2017). The ecological and biogeochemical value of stream network dynamics has been recently highlighted by scientists and policy makers (Abbott et al., 2016; Acuña et al., 2014; Berger et al., 2017; Boodoo et al., 2017; Datry et al., 2014, 2018; Dupas et al., 2019; Durighetto, Bertassello, & Botter, 2022; Giezendanner et al., 2021; Nikolaidis et al., 2013; Reyjol et al., 2014; Vander Vorste et al., 2020; von Schiller et al., 2014), posing a call for hydrology to develop robust empirical or modeling tools for characterizing the spatiotemporal dynamics of surface flow induced by unsteady climate drivers. However, measuring the seasonal and event-based changes in the active portion of stream networks remains impractical in most cases and wet length dynamics have been tracked only in relatively few small catchments across Europe and North America. On the other hand, the availability and the geographical coverage of discharge time series is much higher. In spite of known placement biases of the global river gauge network (Krabbenhoft et al., 2022), within which temporary streams and headwaters might be under-represented, long-term discharge records can be found in a broad range of geographic areas and climatic settings. Therefore, developing tools for linking the total active length that flows upstream of a selected outlet (L) to the surface runoff measured therein (Q_{sur}) represents a promising way to reconstruct active length dynamics of non-perennial rivers capitalizing on widely available recorded streamflow timeseries. A formal link between the actively flowing length of a stream network and the discharge has long been recognized in the literature (Blyth & Rodda, 1973; Day, 1978; Gregory & Walling, 1968). Empirical $L(Q_{sur})$ relations have been often used to quantify the sensitivity of the active length of streams to changes in the underlying hydrological conditions (Durighetto, Mariotto, et al., 2022; Godsey & Kirchner, 2014; Jensen et al., 2017; Lapides et al., 2021; Senatore et al., 2020; Shaw et al., 2017; Ward et al., 2018; Zanetti et al., 2021; Zimmer & McGlynn, 2017).

Recently, the literature has provided a robust conceptual basis to explain the emergence of one-to-one relations between the flowing length of a river and the underlying catchment scale discharge. The conceptual framework (Durighetto & Botter, 2022; Godsey & Kirchner, 2014; Lapides et al., 2021; Prancevic & Kirchner, 2019)

Writing – review & editing: James McNamara, Nicola Durighetto

postulates that surface flow presence depends on the local imbalance between the total inflow and the subsurface outflow in the hyporheic region. More specifically, when the local specific inflow (per unit catchment area) in a given node of the geomorphic river network exceeds the (constant) maximum specific subsurface transport capacity of that node, ρ^*, the corresponding excess water is routed downstream along the network as surface runoff. According to this conceptual model, when the catchment wets up, the specific inflow grows uniformly along the entire network. Consequently, the local subsurface capacity is exceeded in more and more network sites and a larger number of reaches experience surface runoff. Thus, when the catchment wets up and additional water inputs feed the streams through for example, melting, infiltration, exfiltration, soil drainage, the active length of the network and the catchment discharge both increase, originating a monotonically increasing $L(Q_{sur})$ relation.

Starting from the above conceptual scheme, two different types of $L(Q_{sur})$ functions have been proposed in the literature. If ρ^* is assumed to scale with the contributing area as a power law, then the corresponding $L(Q_{sur})$ relation is a power-law as well, that is, $L \propto [Q_{sur}]^b$ with the scaling exponent b being dependent on key morphometric features of the catchment (Prancevic & Kirchner, 2019). When this assumption is relaxed, instead, the $L(Q_{sur})$ law takes the form of the cumulative distribution function of ρ^* along the network, that is, $L \propto CDF_{\rho^*}(Q_{sur})$. The main advantage of the latter formulation lies in its ability to capture S-shaped $L(Q_{sur})$ relations, and its coherence with the concept of a maximum wet length that can't be exceeded even during extreme floods (i.e., for $Q_{sur} \to \infty$).

A major drawback of both the analytical formulations available from the literature, however, is that when discharge at the outlet (Q_{sur}) tends to zero, the upstream flowing length L should approach 0 as well. The limiting behavior of the $L(Q_{sur})$ law for low discharges is particularly important, because during low flows the active length might be extremely sensitive to changes in the catchment discharge (Durighetto & Botter, 2022; Godsey & Kirchner, 2014; Lapides et al., 2021). Nevertheless, low flows can be under-represented in existing data sets for the following reasons: (a) discharge gauging stations are often placed in sections characterized by persistent regimes (*sensu* Botter et al., 2013) with limited streamflow variability; (b) the most intense droughts, during which L approaches 0, might not be captured by short-term or sporadic network mapping campaigns. Although in line with the common intuition, prescribing that $L \to 0$ for $Q_{sur} \to 0$ proves in some cases inappropriate and, in others, an untested assumption. In fact, observed active networks are highly fragmented in most settings (e.g., Godsey & Kirchner, 2014; Goodrich et al., 2018; Perez et al., 2020; Ward et al., 2018; Zimmermann et al., 2014). Thus, if the outlet where discharge is measured is temporarily dry, when the recorded discharge is equal to zero a fraction of the upstream river network could still be actively flowing, that is, $L > 0$ when $Q_{sur} = 0$. Physically, this occurs in all cases in which the active portion of the network retracts in the upstream direction—for example, owing to the presence of a localized spring feeding a losing stream (Durighetto & Botter, 2021). This circumstance indicates that existing $L(Q_{sur})$ relations might not be suited to be applied to temporarily dry outlets. Moreover, as L represents a spatially integrated property of a catchment while Q_{sur} is a point-wise hydrologic signal measured in a pre-defined node of the network, it is unclear to what extent the shape of the $L(Q_{sur})$ relation depends on the specific position of the outlet where the discharge is measured and the size of the contributing catchment. The scaling of the active length versus discharge relation is particularly relevant to understand if (and how) the effect of highly dynamical headwaters is integrated in space when long branching networks with a main perennial channel are considered, and for predicting global-scale temporal variations in the active drainage density of the global river network.

This contribution addresses the above issues by developing a theory that elucidates how current $L(Q_{sur})$ models could be extended to include the case of non-perennial outlets. In particular, we develop three formally distinct analytical expressions of the $L(Q_{sur})$ law that apply to the cases of (a) a perennial outlet; (b) a non-perennial outlet that dries out only when the whole network is dry; and (c) a temporarily dry outlet, that experiences surface flow for less time than other network nodes. The proposed framework is then applied to a set of case studies selected from the literature, to demonstrate the robustness and flexibility of the theory. The manuscript identifies the drivers of potential scale-dependencies in the $L(Q_{sur})$ relation, providing a basis for integrating observed $L(Q_{sur})$ laws in perennial and temporarily dry outlets into a unique mathematical framework.

2. Modeling $L(Q_{sur})$ Laws

2.1. Conceptual Model for Surface Flow Emergence

In this paper, local surface flow presence is described via a water balance approach applied to an arbitrary stream portion of the geomorphic network (Figure 1). The model is that developed by Durighetto and Botter (2022),

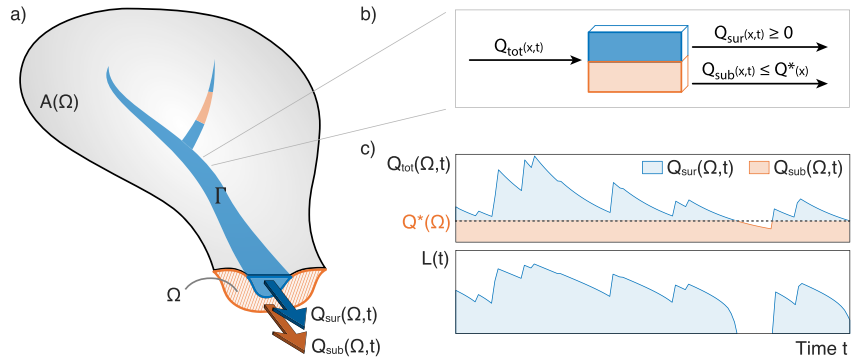

Figure 1. Scheme of the perceptual model proposed in this paper. (a) River catchment defined by the control section Ω, with a dynamic network and a contributing area $A(\Omega)$. In this panel, the geomorphic network (defined as the maximum potential extension of the river network) is indicated as Γ; (b) Schematic of the local water balance that controls surface flow emergence at each location of the network; note that while Q_{sur} and Q_{sub} change through time, Q^* is constant. (c) Example timeseries of flowrate at the outlet, subdivided in surface and subsurface components via the subsurface capacity $Q^*(\Omega)$, and the corresponding active length of the upstream network.

which in turn was built on the concepts previously introduced by Godsey and Kirchner (2014). A crucial element of the formulation is the concept of geomorphic network (hereafter indicated as Γ), defined as the maximum potential extension of the active network in a catchment (see Botter et al., 2021; Zimmer & McGlynn, 2017).

In the proposed formulation, surface flow is assumed to be triggered by the occurrence of saturation excess along the geomorphic network (Dunne & Black, 1970; Tsegaw et al., 2020). Furthermore, network dynamics are seen as a sequence of steady states at different catchment wetness levels, which are quantified by the temporal variations of the discharge in a reference control section (usually the catchment outlet where the discharge is recorded). In particular, the emergence of surface flow within any location of the network is linked to the local imbalance between the flowrate supplied from upstream (intended as the combination of surface discharge, Q_{sur}, and subsurface flow, Q_{sub}) and the maximum subsurface transport capacity of that stream portion, Q^*, as proposed by Godsey and Kirchner (2014) and Prancevic and Kirchner (2019). While Q_{sur} and Q_{sub} change through time in response to precipitation, Q^* is roughly constant, as it is controlled by durable hydro-morphological attributes (e.g., transmissivity, topographic gradient, soil depth as per Prancevic & Kirchner, 2019; Lapides et al., 2021). Surface flow is observed either when the subsurface gets fully saturated by the incoming groundwater flow, or when a fraction of the surface flow produced upstream is delivered downstream as overland flow. Formally, the condition that leads to the local presence of surface flow can be expressed as $Q_{tot} = Q_{sub} + Q_{sur} > Q^*$ (Figure 1b), in line with Godsey and Kirchner (2014); Prancevic and Kirchner (2019); Lapides et al. (2021); Durighetto and Botter (2022). The problem is best formulated using specific quantities (i.e., per unit upslope contributing area). This requires the definition of the local specific discharge, $q_{tot}(x, t) = Q_{tot}(x, t)/A(x)$, and the local subsurface discharge capacity $\rho^*(x) = Q^*(x)/A(x)$, $A(x)$ being the upslope contributing area at the location x. The presence/absence of surface flow at a given location of the network (x) is thus expressed by the following equation:

$$X(x,t) = \begin{cases} 1 & \text{if } q_{tot}(x,t) > \rho^*(x) \\ 0 & \text{otherwise} \end{cases} \quad (1)$$

where $X = 1$ implies the presence of flowing water and $X = 0$ corresponds to a dry riverbed in the relevant cross section (Botter & Durighetto, 2020). In the above equation, $\rho^*(x)$ is a spatially variable threshold for the local specific inflow $q_{tot}(x, t)$, above which surface flow is observed. $\rho^*(x)$ thus represents the specific subsurface flow experienced by the location x during all the times in which surface flow is observed.

2.2. General Relation Between Active Length L and Total Flowrate Q_{tot}

Characterizing the spatial and temporal patterns of $q_{tot}(x, t)$ within Γ might be difficult, as the total inflow along the geomorphic network can not be measured. Here, we assume that $q_{tot}(x, t)$ can be expressed as $q(t)\ \alpha(x)$, where

$\alpha(x)$ is a dimensionless factor that defines the spatial variations of the specific discharge along the network. The above formulation implies that the spatial and temporal variations of $q_{tot}(x, t)$ can be decoupled (i.e., the ratio between the inflow at two different points of the network does not change in time as the discharge varies, and it is only dependent on $\alpha(x)$). Under the above assumption, the local flowrate at the outlet ($x = \Omega$), $Q_{tot}(\Omega, t)$, can be expressed as $Q_{tot}(\Omega, t) = A(\Omega)\alpha(\Omega)q(t)$, $A(\Omega)$ being the contributing area of the whole catchment. The pattern of $\alpha(x)$ along the network can be defined save for a constant factor, which is here conveniently embedded in $q(t)$. Thus, the specific discharge observed in the position $x \in \Gamma$, $q_{tot}(x, t)$, can be estimated without loss of generality setting $\alpha(\Omega) = 1$ and combining the above equations as:

$$q_{tot}(x, t) = \frac{\alpha(x) Q_{tot}(\Omega, t)}{A(\Omega)}. \tag{2}$$

According to Equation 2, the catchment discharge $Q(\Omega, t)$ and $q_{tot}(x, t)$ do change with time in a synchronous manner in response to wetting and drying cycles linked to precipitation and climate dynamics.

In the proposed framework, the total length of the active network at a given time can be obtained by integrating the status of each point $X(x, t)$, as given by Equation 1, along the geomorphic network:

$$\begin{aligned} L(t) &= \int_{\Gamma} X(x,t)dx = \int_{\Gamma} H\left[q_{tot}(x,t) - \rho^*(x)\right]dx = \\ &= \int_{\Gamma} H\left[\frac{Q_{tot}(\Omega,t)}{A(\Omega)} - \frac{\rho^*(x)}{\alpha(x)}\right]dx = L_g\, CDF_{r^*}\left[\frac{Q_{tot}(\Omega,t)}{A(\Omega)}\right], \end{aligned} \tag{3}$$

where $H[\cdot]$ is the Heaviside step function, L_g is the length of the geomorphic network, $r^*(x) = \rho^*(x)/\alpha(x)$ and CDF_{r^*} indicates the Cumulative Distribution Function (CDF) of r^*—which implicitly accounts for the spatial variations of q_{in} along the network and is conceived here as a spatial random variable. The total network length is calculated as the sum of all the lengths associated to the active sites of the network, that is, the nodes where $X(x, t) = 1$. The right-hand side of the first line of Equation 3 expresses the condition necessary for flow emergence ($X = 1$), as dictated by Equation 1. Then, in the second line of Equation 3, $q_{tot}(x, t)$ is expressed as a function of $Q_{tot}(\Omega, t)$ as per Equation 2 to separate space and time dependencies. Consequently, the integral over $x \in \Gamma$ can be replaced by an integral over $r^* \in (0, \infty)$, which is embedded into the cumulative distribution of r^*, CDF_{r^*}.

Equation 3 is analogous to Equation 8 in Durighetto and Botter (2022), but relaxes two key assumptions: (a) the spatial uniformity of the inflow q_{in} along the network (which is here overcome by replacing ρ^* with r^*); and (b) the equality between the total flowrate at the outlet and the corresponding surface runoff (i.e., $Q_{tot}(\Omega, t) = Q_{sur}(\Omega, t)\ \forall\ t$). With this regard, Equation 3 clarifies that the active length L depends on the total discharge at the outlet $Q_{tot}(\Omega, t)$, and not just on the surface component of it as implicitly assumed by current $L(Q)$ models. While in perennial outlets it is reasonable to assume that $Q_{sub}(\Omega, t) \ll Q_{sur}(\Omega, t)$, this is not the case if the cross section where discharge is measured temporarily dries out ($Q_{sur}(\Omega, t) \to 0$). The above derivation thus provides the rationale to explain why current analytical models that link the active length to the observed surface runoff might fail in reproducing the behavior of dynamically fragmented river networks if the outlet dries out.

Provided that the local status of each network portion varies in time as a function of $q_{tot}(x, t) \propto Q_{tot}(\Omega, t)$, a one-to-one monotonic relation between $Q_{tot}(\Omega, t)$ and the corresponding wet length arises from Equation 3. According to the proposed model, when $Q_{tot}(\Omega, t)$ falls below the minimum value of $[\rho^*(x)A(\Omega)]/\alpha(x)$ along the geomorphic network, the active length approaches zero. In such circumstances, in fact, the least persistent node of the network can no longer sustain surface flow and the network completely dries out. Therefore, the function $L(Q_{tot}(\Omega))$ shall approach the x-axis not only for $Q_{tot}(\Omega) \to 0$, but—more likely—for a strictly positive value of $Q_{tot}(\Omega)$.

Equation 3 can be used as a basis to describe $L(Q)$ relations in the general case, regardless of the fraction of time during which the outlet experiences surface runoff. However, Q_{tot} is quite difficult to measure in the filed, as the longitudinal subsurface component of the total discharge can be captured by existing gauging techniques only in very few circumstances, for example, in the presence of control structures that limit the magnitude of bypass flows or when salt dilution methods are used in streams with very high bed permeability (Seybold et al., 2023). Furthermore, also in these cases it is not known a priori to what extent subsurface flows are actually captured, a circumstance that enhances the uncertainty associated with the observations of the total discharge, Q_{tot}. Therefore,

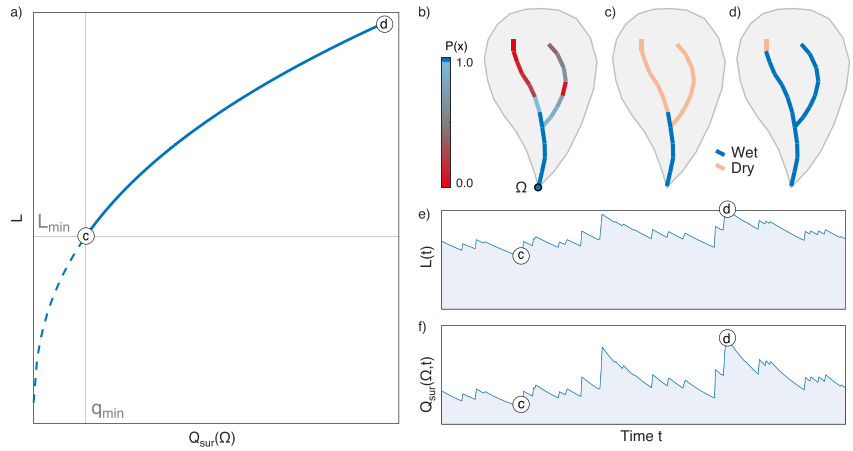

Figure 2. (a) $L(Q_{sur})$ relation in a catchment with perennial outlet; circles c and d refer to the networks depicted in panels (c) and (d), respectively. (b) Spatial distribution of local persistency $P(x)$, defined as the relative fraction of time during which the location x experiences surface runoff (in analogy with the definition of $P(\Omega)$ given by Equation 4); (c) active network at the minimum extent; (d) active network at the maximum extent; (e) and (f) timeseries of active length and surface flow at the outlet, respectively.

there is a practical need to transform the $L(Q_{tot}(\Omega))$ relation given by Equation 3 into an equivalent—and more useful—$L(Q_{sur}(\Omega))$ relation which could be applied to all the cases in which only the surface component of the total discharge is known. To this aim, quantitative information on the degree of persistence of the outlet is needed. The persistence of the outlet, $P(\Omega)$, is defined as the percentage of time for which the outlet experiences surface flow (i.e., the expected value of $X(\Omega, t)$), and can be empirically computed as:

$$P(\Omega) = \text{Prob}_t \left[Q_{tot}(\Omega, t) > Q^*(\Omega) \right]. \tag{4}$$

In the following, we derive the relationship between L and $Q_{sur}(\Omega)$ for $P(\Omega) = 1$ and $P(\Omega) < 1$ into two separate subsections. For the sake of illustration, hereafter it is assumed that $\alpha(x) = \alpha(\Omega) = 1\ \forall x$, so as $r^*(x) = \rho^*(x)\ \forall x$. The full set of equations corresponding to the case in which $\alpha(x)$ is not constant can be found in the Supporting Information S1.

2.3. $L(Q_{sur})$ Relation in Case of Perennial Outlets

If $Q_{tot}(\Omega, t) > Q^*(\Omega)\ \forall t$, the catchment outlet is perennial ($P(\Omega) = 1$), and never dries out (see example in Figure 2). As the persistence of the outlet is 1, one can reasonably assume that $Q_{sur}(\Omega, t) \simeq Q_{tot}(\Omega, t)\ \forall t$, as long as surface transport is much more efficient than the corresponding subsurface flow. Thus, Equation 3 can be rewritten as follows:

$$L(Q_{sur}(\Omega)) = L_g\, CDF_{\rho^*}\left[\frac{Q_{sur}(\Omega)}{A(\Omega)}\right], \tag{5}$$

where CDF_{ρ^*} indicates the spatial CDF of $\rho^*(x)$. Provided that the minimum observed value of $Q_{sur}(\Omega, t)$, say $Q_{sur,min}(\Omega)$, is strictly positive, the behavior of the $L(Q_{sur}(\Omega))$ relation for $Q_{sur}(\Omega) \to 0$ can not be experimentally observed (Figure 2a), as only the upper-rightmost portion of the $L(Q)$ law is visible, that is, the part of the curve for $Q_{sur}(\Omega) > Q_{sur,min}(\Omega)$ and $L > L_{min} = L_g CDF_{\rho^*}\left[\frac{Q_{sur,min}(\Omega)}{A(\Omega)}\right]$. The lower-left part of the $L(Q_{sur}(\Omega))$ curve, instead, could be revealed only by intense droughts that could make the catchment experience a wetness degree that is lower than the driest state in correspondence of which $Q_{sur}(\Omega)$ and L were recorded. This case is schematically represented in Figure 2, where we have represented the joint dynamics of L and Q in an idealized catchment (panels e and f), and the configuration of the active network observed in correspondence of the minimum (panel c) and the maximum (panel d) degree of wetness experienced by the catchment, in agreement with the spatial patterns of local persistency (panel b). This case comprises most of the sections for which synchronous active length and discharge data are available in the literature. However, it should be noted that, in some cases, the minimum value of $Q_{sur}(\Omega)$—though strictly positive—can be very low, making the assumption $Q_{sur}(\Omega, t) \simeq Q_{tot}(\Omega,$

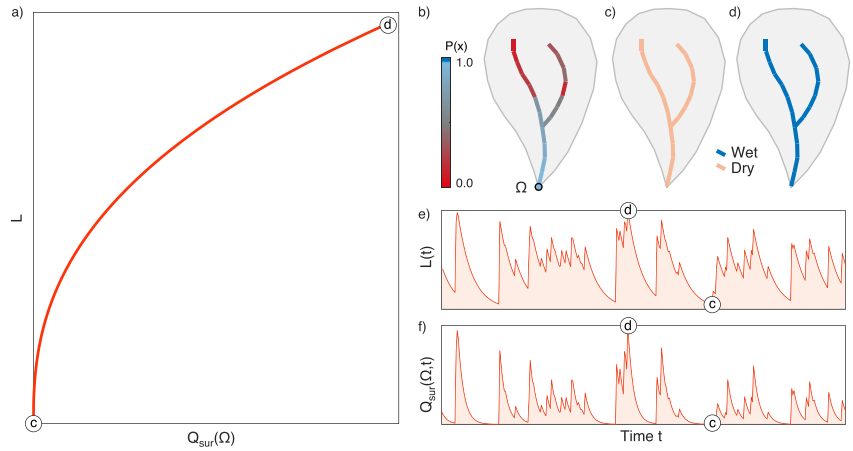

Figure 3. (a) $L(Q_{sur})$ relation in a catchment with a temporarily dry outlet; circles c and d refer to the networks depicted in panels (c) and (d), respectively. (b) Spatial distribution of local persistency, $P(x)$, defined as the relative fraction of time during which the location x experiences surface runoff (in analogy with the definition of $P(\Omega)$ given by Equation 4). In this case, the outlet is the most persistent location of the whole network, as observed in cases where streamflow generation is a spatially homogeneous process and the persistency is proportional to the contributing area; (c) active network at the minimum extent; (d) active network at the maximum extent; (e) and (f) timeseries of active length and surface flow at the outlet, respectively.

t) no longer valid. Under the above circumstances, one should employ the equations derived in the following section, which addresses the case of a temporarily dry outlet.

2.4. $L(Q_{sur})$ Relations in Case of Temporarily Dry Outlets

If the selected outlet is temporarily dry (i.e., $P(\Omega) < 1$), then $Q_{sub}(\Omega, t) < Q^*(\Omega)$ at least for some values of t. The control section, in fact, dries out at times because the local inflow at the outlet can not sustain surface flow all-year round. In this case, when the outlet experiences surface runoff, $Q_{sur}(\Omega, t)$ is the difference between $Q_{tot}(\Omega, t)$ and $Q^*(\Omega)$. Otherwise, the total inflow is only made up by subsurface flow:

$$Q_{tot}(\Omega,t)=\begin{cases} Q_{sur}(\Omega,t)+Q^*(\Omega) & \text{if } Q_{sur}(\Omega,t)>0 \\ Q_{sub}(\Omega,t)>0 & \text{if } Q_{sur}(\Omega,t)=0 \end{cases} \tag{6}$$

Equation 6 indicates that when $Q_{sur}(\Omega) > 0$, $Q_{tot}(\Omega)$ and $Q_{sur}(\Omega)$ differ by a positive constant, $Q^*(\Omega)$, which is dependent on the local hydromorphologic features of the outlet. Therefore, Equation 3 can be rewritten as:

$$L(Q_{sur}(\Omega))=L_g\,CDF_{\rho^*}\left[\frac{Q_{sur}(\Omega)+Q^*(\Omega)}{A(\Omega)}\right], \tag{7}$$

which expresses the general relationship between L and $Q_{sur}(\Omega)$. Owing to the hierarchical nature of network dynamics (sensu Botter et al., 2021) implied by Equations 1 and 2, if the outlet is the most persistent section of the entire geomorphic river network (see Figure 3), then all the river network is dry whenever $Q_{sur}(\Omega) = 0$ (panel c and point c in panels a, e and f in Figure 3). Under the above circumstances, $\rho^* = Q^*/A$ takes a minimum value at the outlet Ω (e.g., because the contributing area is maximum therein), and the following condition applies:

$$CDF_{\rho^*}\left[\frac{Q^*(\Omega)}{A(\Omega)}\right]=0, \tag{8}$$

where CDF_{ρ^*} is interpreted as the non-exceedance probability of $\rho^*(x)$. In such a case, when the outlet is dry (i.e., $Q_{sur}(\Omega, t) = 0$), the local inflow is lower than the subsurface capacity in all the nodes of the network (i.e., $q_{tot}(x,$

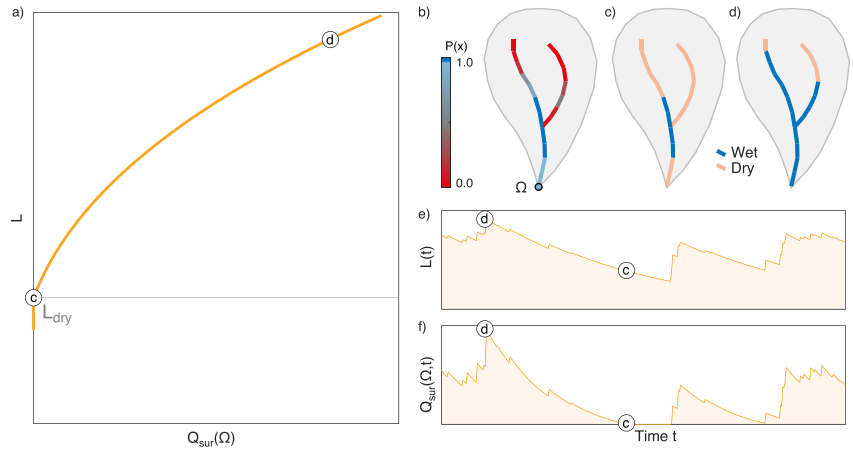

Figure 4. (a) $L(Q_{sur})$ relation in a catchment with a temporarily dry outlet, which however is not the most persistent node in the network; circles c and d refer to the networks depicted in panels (c) and (d), respectively. (b) Spatial distribution of local persistency, $P(x)$, defined as the relative fraction of time during which the location x experiences surface runoff (in analogy with the definition of $P(\Omega)$ given by Equation 4). In this case, the outlet is not the last node to dry out in the network; (c) active network at the minimum extent; (d) active network at the maximum extent; (e) and (f) timeseries of active length and surface flow at the outlet, respectively.

$t) < \rho^*(x)\ \forall\ x)$, thereby implying that the total active length is zero (i.e., $L = 0$). Consequently, Equation 7 can be rewritten as (see Supporting Information S1):

$$L(Q_{sur}(\Omega)) = L_g\, CDF_{\Delta\rho^*}\left[\frac{Q_{sur}(\Omega)}{A(\Omega)}\right], \tag{9}$$

where $\Delta\rho^*(x) = \rho^*(x) - \rho^*(\Omega)$ is the excess specific subsurface capacity of the site x with respect to that of the outlet ($\rho^*(\Omega)$, which is the minimum value of ρ^* along the whole network). The functional form of the $L(Q_{sur})$ relation implied by Equation 9 is thus the same as that obtained for persistent outlets (Equation 5), the only difference being that in this case the reference physical quantity involved is the excess of specific discharge capacity with respect to the outlet, $\Delta\rho^*$, instead of ρ^* itself. Therefore, according to Equation 9, as the minimum value of $\Delta\rho^*(x)$ in Γ is zero, when $Q_{sur}(\Omega) = 0$ also the flowing length of the network is zero (i.e., $L(Q_{sur}(\Omega)) = 0$ when $Q_{sur}(\Omega) = 0$, see Figure 3a). Note that the same equation can be applied also to the cases in which the outlet is perennial but it experiences very low flows (i.e., $Q^*(\Omega) > Q_{sur,min}(\Omega)$) and during the most intense droughts the large majority of the network disappears $\left(CDF_{\rho^*}\left[\frac{Q_{sur,min}(\Omega)}{A(\Omega)}\right] \ll L_g\right)$.

In the above circumstances, existing $L(Q_{sur})$ models can still be used to represent observed L versus Q_{sur} patterns, as they allow one to describe how both L and Q_{sur} get close to zero when the network dries out. The only theoretical inconsistency in applying traditional $L(Q_{sur})$ laws to temporary outlets of this type (i.e., $P(\Omega) < 1$ but $P(\Omega) > P(x)\ \forall x \in \Gamma$) is that $\Delta\rho^*$ is physically misinterpreted as ρ^*. Provided that neither $\Delta\rho^*$ or ρ^* can be directly measured, however, this shortcoming does not have significant practical drawbacks when the fitting of observed L versus Q_{sur} points is concerned. Note that in this case, the full shape of the $L(Q_{sur})$ relation can be potentially reconstructed exploiting field data, as the network dries out completely (as in the example presented in Figure 3).

On the other hand, if the outlet is temporary but is not the last section of the whole network to dry (Figure 4), when $Q(\Omega, t) = 0$ the total inflow $Q_{tot}(\Omega, t)$ is still positive, and some upstream sections of the network are flowing even though the outlet is dry (Figure 4c). Under the above circumstances Equation 7 applies, but in this case the upstream flowing length L is strictly positive even for $Q_{sur} \to 0$ (see point c in Figures 4e and 4f) and this minimum flowing length—that is observed when the outlet is dry—is equal to:

$$L_{dry} = L_g CDF_{\rho^*}\left[\frac{Q^*(\Omega)}{A(\Omega)}\right] > 0. \tag{10}$$

Therefore, Equation 7 can not be simplified to Equation 9. Moreover, given the non-perennial nature of the outlet, only the part of the $L(Q_{sur})$ relation in the domain $L > L_{dry}$ can be empirically observed, while the lower-left part of the curve would require information on the discharge in a more persistent section of the catchment.

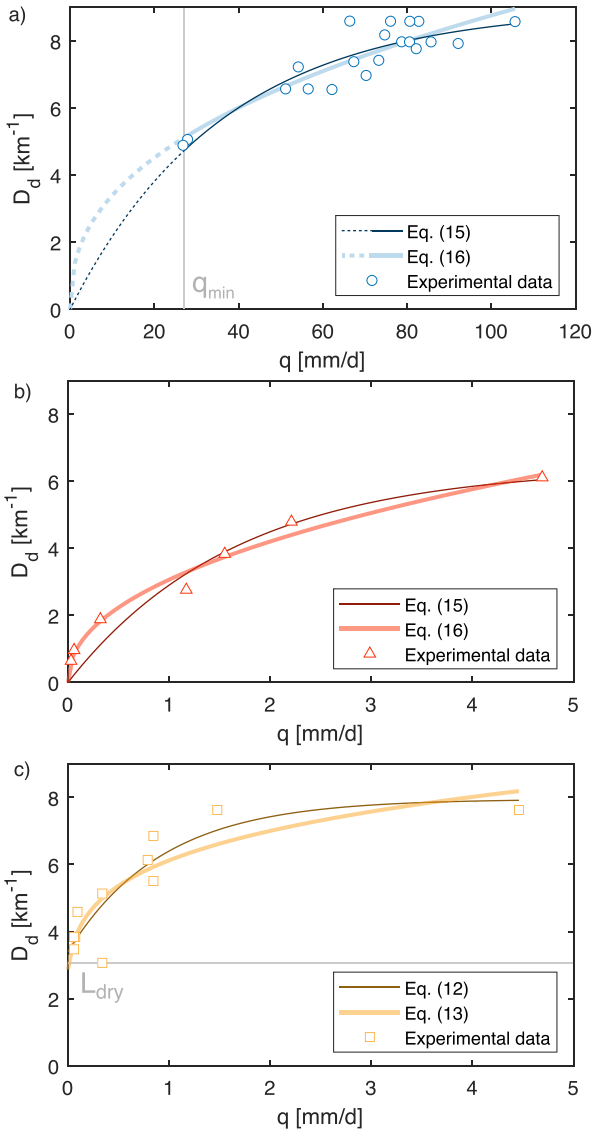

Figure 5. Relations between drainage density D_d and specific discharge q in three example experimental catchments: (a) Burnaby (Roberts & Archibold, 1978), which represents the case of a perennial outlet; (b) Poverty creek (Jensen et al., 2017), which represents the case of a non-perennial outlet that dries out only when the whole upstream network is dry; and (c) Turbolo creek (Botter et al., 2021; Senatore et al., 2020), which represents the case of a temporarily dry outlet, that experiences surface flow for less time than other network nodes (see Table S2 in Supporting Information S1). Equations 15 and 16 have been fitted to the available data in panels a and b, while Equations 12 and 13 have been fitted to the empirical data in panel (c). The fitted parameters are reported in Table S3 in Supporting Information S1.

In this case, the currently available models that link L to Q_{sur} are no longer suited to describe the co-evolution of L and Q_{sur}, as they assume that $L \to 0$ for $Q_{sur} \to 0$.

3. Proof-Of-Concept Application

In the previous sections we have discussed the reasons why three formally distinct expressions for the $L(Q_{sur})$ relationship exist, depending on the persistency of the outlet: Equation 5, when the outlet is perennial; Equation 7, when the outlet is temporarily dry, but it is not the last node of the network to dry out; and Equation 9, when the outlet is temporarily dry but it dries out only when the whole network is dry.

The most general formulation is that given by Equation 7, which can be rewritten as a function of the specific discharge observed at the outlet (by unit contributing area), $q_{sur}(\Omega)$, as:

$$L = L_g \, CDF_{\rho^*}\left[q_{sur}(\Omega) + \rho^*(\Omega)\right], \tag{11}$$

The formula requires the use of at least three parameters: (a) the maximum length of the network, L_g (which however can be determined empirically by field surveys); (b) the specific subsurface discharge capacity of the cross section where the discharge is measured, ρ^*; and (c) the parameter(s) defining the CDF of ρ^* along the network (at least one). For instance, if the CDF of ρ^* is exponential, the number of parameters of the general model represented by Equation 11 is minimum (only three), and the $L(Q)$ relation can be rewritten as:

$$L = L_g \exp\left[-k(q_{sur}(\Omega) + \rho^*(\Omega))\right], \tag{12}$$

where k is the reciprocal of the mean value of ρ^* along the network. Likewise, if the CDF of ρ^* is assumed to be a power-law, then Equation 11 reads:

$$L = a\left[q_{sur}(\Omega) + \rho^*(\Omega)\right]^b, \tag{13}$$

where the scaling constant a embodies the geomorphic drainage density L_g. Equation 13 generalizes the power-law model commonly used in the literature. If the local persistency observed at the outlet is the maximum value along the network, Equation 11 can be simplified to:

$$L = L_g \, CDF_{\Delta\rho^*}[q_{sur}(\Omega)], \tag{14}$$

in which $\Delta\rho^* \simeq \rho^*$ whenever the outlet is perennial (i.e., $P(\Omega) = 1$ and $\rho^*(\Omega) \to 0$). Equation 14 can be further specified using the exponential or the power-law models as:

$$L = L_g \exp[-k \cdot q_{sur}(\Omega)]; \tag{15}$$

$$L = a[q_{sur}(\Omega)]^b. \tag{16}$$

The latter equations, however, can be used only if the control section where the discharge is measured is the section with the highest persistency among all the nodes belonging to the observed stream network. This also includes the case of a temporarily dry outlet (Equation 7) and that of a perennial outlet (Equation 5). However, if the outlet is perennial, the left part of the curve can be poorly constrained by the observations, as the active network never dries out completely.

Figure 5 exemplifies the diversity of shapes emerging in the $L(Q)$ relations built from experimental data gathered in different regions of the world, in line with what foreseen by the general theory presented in this paper. Note that the empirical data presented here have the only purpose of demonstrating the variety of possible shapes in

the empirical relation between the total flowing length and the catchment discharge. Consequently, technical issues such as the fitting of analytical CDFs to the data, and the presence of hysteresis in the $L(Q)$ plots are not discussed, as they fall outside the scope of the present paper. For the sake of illustration, Figure 5 reports the relationship between L and $q_{sur}(\Omega)$ in three catchments: the Burnaby (Roberts & Archibold, 1978), Turbolo (Botter et al., 2021), and Poverty (Jensen et al., 2017) (see Table S1 in Supporting Information S1). The selected case studies correspond to the three classes of $L(Q_{sur})$ relations identified in this paper, namely (a) the case of a perennial outlet (Figure 5a); (b) the case of a non-perennial outlet that dries out only when the whole upstream network is dry (Figure 5b); and (c) the case of a temporarily dry outlet, that experiences surface flow for less time than other network nodes Figure 5c). In the Burnaby catchment (shown in Figure 5a), the $L(Q)$ law has been evaluated in a perennial outlet (i.e., $P(\Omega) = 1$), thereby implying that the shift between $Q_{sur}(\Omega)$ and $Q_{tot}(\Omega)$ can be neglected. Consequently, Equations 15 and 16 can be applied to fit the observed data of L and Q_{sur}. The experimental points clearly indicate that in this case the lower left part of the curve (dotted and dashed lines) is not revealed by the empirical data, provided that the fraction of channel length that is always observed as active is not-negligible. This is not the case for the Poverty catchment (Figure 5b), which dries out almost completely, thereby enabling a detailed reconstruction of the full shape of the $L(Q)$ relationship—as almost all the nodes in the network have a persistency lower than 1. The $L(Q)$ relation in the Turbolo catchment, instead, has a completely different shape (Figure 5c), as in this case L does not decrease to zero as the discharge at the outlet decreases. This indicates that in the Turbolo catchment the outlet is not the most persistent node of the network. This behavior is due to the presence of a localized spring located in the middle portion of the network which feeds a losing channel. This instance generates a significant leftward shift in the $L(Q_{sur})$ relation, which is dependent on the unknown value of $Q^*(\Omega)$.

The fitting examples presented in the above paragraphs offer the opportunity to discuss how much data are needed to build reliable $L(Q_{sur})$ relations, and whether the available data are sufficient to distinguish among the three models proposed in this paper. When one tries to reconstruct the shape of the $L(Q_{sur}(\Omega))$ law in a catchment, it is particularly useful to measure the maximum possible extent of the network, that is, the geomorphic network length, L_g. The importance of estimating the geomorphic network stems not only from the ability to identify the behavior of the $L(Q_{sur})$ curve for high discharges, but also from the fact that L_g explicitly appears in most of the general equations derived in this paper (e.g., Equations 11 and 14). To estimate L_g two different methods are available: (a) mapping the active network length at a random time, and adding on top of this length the longitudinal extent of the regions of the landscape where signs of permanent channelization can be detected (e.g., Durighetto et al., 2020); (b) observing the active network in correspondence of a very high flow. Importantly, L_g can't be estimated a priori from a digital terrain map, as the threshold for the extraction would be unknown. However, the estimate of L_g could be potentially done through a single survey. When the geomorphic channel length is known, other surveys are necessary to evaluate the flowing length corresponding to a range of different discharge conditions, down to $Q_{sur} \to 0$. In principle, just a few pairs of L and Q_{sur} observations could be strictly necessary to fit some analytical model to the data (at least as much observations as the total number of parameters in the analytical model). However, getting more data is important, especially if the outlet is not the last node to dry out in the network (a circumstance which increases the number of parameters at play). In fact, observed $L(Q_{sur})$ relations can exhibit some scattering (Jensen et al., 2019; Zanetti et al., 2021), which potentially hinders the behavior of the $L(Q_{sur})$ law when the amount of empirical information is limited. Moreover, the shape of the $L(Q_{sur})$ relations can be very complex, owing to the presence of knees, changes in the concavity and plateaus. Therefore, the availability of empirical data on active length and discharge in a limited range of discharges (e.g., mostly under high flow conditions) can lead to biased estimates of the model parameters. With this regard, it is important to emphasize the key role of low flows to determine the behavior of the $L(Q_{sur})$ relation close to the origin and to identify the most appropriate functional form for the $L(Q_{sur})$ relation (e.g., by determining whether the shifting factor $\rho^*(\Omega)$ needs to be taken into account or not). As a general rule of thumb, we propose that 5 to 10 points in the $L(Q_{sur})$ plane gathered under different flow conditions (including very low flows) should represent a good basis to estimate the shape of the relationship between active length and catchment discharge in most settings.

4. Implications, Extensions and Scaling Issues

The three behaviors discussed in Sections 2.3 and 2.4 and depicted in Figure 5 identify three different functional forms for the $L(Q_{sur})$ relation. However, it is important to highlight that all these equations originate from the same curve, namely the spatial CDF of the specific subsurface capacity. In fact Equations 5, 7, and 9 all represent translations/truncations of Equation 3, the shape of which depends on morphological and hydrological features

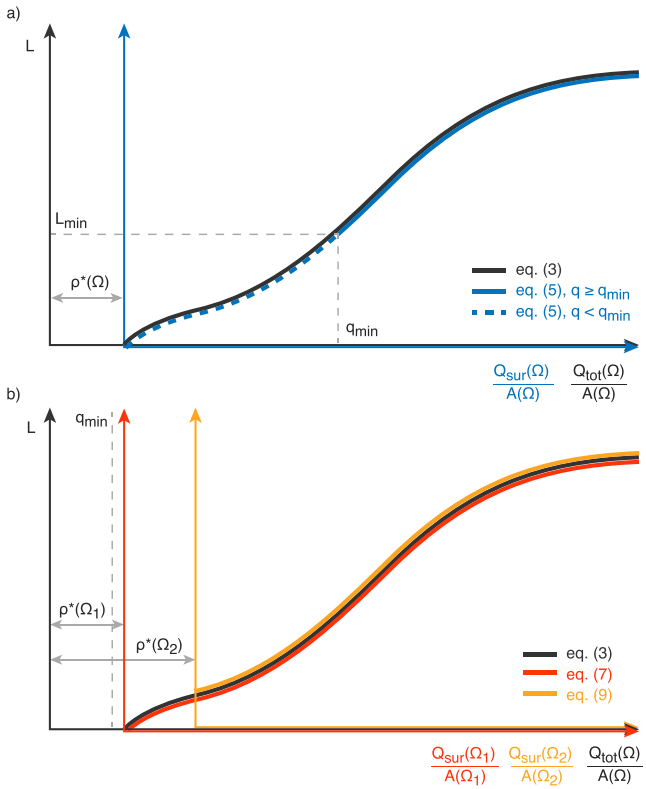

Figure 6. Summary of the three possible shapes of $L(Q_{sur})$. (a) case with perennial outlet and the corresponding $L(Q_{tot})$ relation; (b) cases with temporarily dry control section.

in the hyporheic region along the network (Dohman et al., 2021; Durighetto & Botter, 2022; Godsey & Kirchner, 2014; Lapides et al., 2021; Prancevic & Kirchner, 2019). This is graphically represented in Figure 6, in which we show the relationship between the $L(Q_{tot}(\Omega))$ as given by Equation 3 and the corresponding $L(Q_{sur}(\Omega))$ laws emerging in the cases of: (a) a perennial outlet (panel (a); (b) a temporary outlet with the maximum value of persistency along the whole network (panel b, section Ω_1) and (c) a temporary outlet with a persistency which is not the highest value of P along the geomorphic network (panel b, section Ω_2). For the sake of illustration, in this figure Ω, Ω_1 and Ω_2 identify generic discharge control sections located along the geomorphic network, and not necessarily the catchment outlet (which is considered to be fixed). Within this formulation, the role of the control section is that of allowing a quantitative assessment of the dynamics of the specific discharge by unit catchment area along the network, $q_{tot}(x, t)$, using the observed time-series of $Q_{sur}(\Omega)$—as per Equation 2. This caveat will enable us to virtually "change" the position of the control section along the network, without changing the geomorphic network Γ and the spatial distribution of ρ^* along the network (black curve in Figure 6). Figure 6a refers to the case in which the minimum specific discharge in the control section, $q_{sur,min}(\Omega) = Q_{sur,min}(\Omega)/A(\Omega)$ is much larger than the specific subsurface capacity of the control section itself, which implies that $P(\Omega) = 1$. In this case the shift between the two curves $L(Q_{tot}(\Omega))$ and $L(Q_{sur}(\Omega))$ is small as compared to the values of $q_{sur}(\Omega, t)$ at play, and thus can be neglected. Therefore, the standard models found in the literature can be applied to interpret and describe the observed $L(Q_{sur}(\Omega))$. However, the $L(Q)$ law might not be fully visible in empirical data because the specific discharge variations along the network can not unveil the potential dynamics of the node(s) in the network with the lowest values of ρ^* (which are the last to dry out during recessions). Conversely, Figure 6b refers to the case in which the minimum specific discharge in the control section, $q_{sur,min}(\Omega)$ is lower than the minimum value of the specific subsurface capacity along the network, which implies that $P(\Omega) < 1$, regardless of the position of the control section along Γ (i.e., the active network completely dries out at times). In this case, the shift between the $L(Q_{tot}(\Omega))$ and the $L(Q_{sur}(\Omega))$ curves can't be neglected, an instance which might challenge the use of existing $L(Q)$ models. However, if the control section is selected in the point of the network with the maximum persistency (outlet Ω_1), then the standard models—according to which $L \to 0$ if $Q_{sur} \to 0$—can be used (red curve) provided that they are re-interpreted in terms of the CDF of $\Delta\rho^*(x)$ (i.e., the excess of specific subsurface capacity as compared to that of the outlet). In this case, the full shape of the $L(Q)$ relation is visible, precisely because the network completely dries out. However, if the control section (Ω_2) is not the node of the network with the highest value of the persistency (i,e, minimum value of ρ^*), the $L(Q_{tot})$ relation gets truncated when translated into the equivalent $L(Q_{sur})$ relation (orange curve). This left truncation is controlled by the difference between the maximum value of P along the network and $P(\Omega)$, and emerges from the fact that the selected control section (where Q_{sur} is measured) can not be used to track the temporal variations of q_{tot} in some nodes of the network—namely all the nodes with a persistency lower than $P(\Omega)$.

This analysis clarifies that the shape of the $L(Q)$ relation is controlled by the spatial CDF of the maximum specific subsurface capacity of the hyporheic region along the geomorphic network, with an unknown shifting factor (i.e., $\rho^*(\Omega)$) that comes into play when the outlet is not the most persistent section of the network. To circumvent the need for specifying this unknown shifting factor, the discharge control section could be placed in perennial outlets, so as to eliminate left-truncation effects. However, it is not necessarily true that placing the discharge gauging station in a "downstream" section with a relatively large contributing area is the optimal strategy to unveil the full shape of the $L(Q)$ law in all cases. In fact, if the outlet is placed in a section with a very large drainage area (such that the persistency of the outlet increases to 1), the lower-left part of the $L(Q)$ relation might become invisible (climate-driven veiling), since in the latter case not only the outlet but also a significant part of the network could be perennial. In real-world river basins, when the control section is moved downstream and the corresponding contributing area increases, not only the persistency of the outlet $P(\Omega)$ is likely to increase

(since ρ^* generally decreases in the downstream direction driven by the increase of contributing area), but also the statistical distribution of ρ^* inevitably changes, since a larger number of perennial nodes are progressively included in the geomorphic network. This seems to suggest that the shape of the $L(Q)$ relation could be inevitably scale dependent. This scaling is induced by the following two intertwined mechanisms: (a) the spatial variations of the cumulative distribution of ρ^* across scales; (b) the changes in the magnitude of the left truncation and climate-driven veiling effects with the increasing contributing area (see above). Still, it could be possible that at some point, when the size of the catchment is sufficiently large, the shape of CDF_{ρ^*} become scale-invariant, owing to the compensation effect generated by the aggregation of multiple dynamical headwater catchments around a perennial network. However, this hypothesis is difficult to verify or falsify at this stage, given the limited capabilities of currently available technological tools to map stream network dynamics at large scales with sufficient temporal and spatial resolutions.

We propose that the active length—discharge relation represents a useful tool to analyze how climate fluctuations can impact the structure of the flowing network, and to identify the full array of geomorphic footprints in the hydrological response of rivers—beyond the classical geomorphological theory of the hydrological response that relies on a fixed channel network structure (e.g., Rodriguez-Iturbe et al., 1998).

5. Conclusions

In this paper, we have derived three formally distinct analytical expressions to describe the relationship between the total wet length of rivers and the underlying catchment discharge, which refer to the cases of (a) a perennial outlet; (b) a non-perennial outlet that dries out only when the upstream network is dry and (c) a temporarily dry outlet, that dries out before some other upstream nodes. Our derivation demonstrates that, under the assumptions done in this paper, in all cases the shape of $L(Q_{sur})$ relation is controlled by the CDF of the specific subsurface discharge capacity along the network. Our results indicate that in general the relation between L and Q_{sur} has at least three parameters, including an unknown shifting factor which corresponds to the specific subsurface capacity of the outlet, $\rho^*(\Omega)$. The above shifting factor can be operationally neglected in a number of common circumstances (e.g., perennial outlets), but has a significant impact on the observed $L(Q_{sur})$ laws if the discharge gauging station is not located in the most persistent node of the whole network (as might be observed in dynamically fragmented river networks). We also provided a set of real-world examples built using experimental data gathered in three different field sites, in which the observed $L(Q_{sur})$ laws follow the three prototypical behaviors identified by the proposed theory. Our results clarify that the whole shape of the $L(Q_{sur})$ relation is driven by hydro-morphological features of the hyporheic region connected to the river network, but its empirical reconstruction can be difficult in the following circumstances: (a) if the maximum specific subsurface capacity of the channels where the discharge control section is placed is too low, which implies that a significant fraction of the network is perennial; (b) if the persistency of the node where the discharge is measured is not the maximum persistency of the network, which implies that other nodes in the network experience surface flow for longer than the discharge gauging station. The study provides a basis for integrating empirical data about the joint dynamics of discharge and active length gathered in catchments characterized by contrasting size, climate and geomorphological features into a coherent mathematical framework.

Data Availability Statement

All the empirical data used in this study is publicly available at the Durighetto and Botter (2023) repository, named *Extending active network length versus catchment discharge relations to temporarily dry outlets*, link https://doi.org/10.25430/researchdata.cab.unipd.it.00000912.

Acknowledgments
This research was supported by the European Community's Horizon 2020 Excellent Science Programme (Grant H2020-EU.1.1.-770999). Detailed methods can be found in the Supporting Information (Text S1 to S3 in Supporting Information S1).

References

Abbott, B. W., Baranov, V., Mendoza-Lera, C., Nikolakopoulou, M., Harjung, A., Kolbe, T., et al. (2016). Using multi-tracer inference to move beyond single-catchment ecohydrology. *Earth-Science Reviews*, *160*, 19–42. https://doi.org/10.1016/j.earscirev.2016.06.014

Acuña, V., Datry, T., Marshall, J., Barceló, D., Dahm, C. N., Ginebreda, A., et al. (2014). Why should we care about temporary waterways? *Science*, *343*(6175), 1080–1081. https://doi.org/10.1126/science.1246666

Berger, E., Haase, P., Kuemmerlen, M., Leps, M., Schäfer, R. B., & Sundermann, A. (2017). Water quality variables and pollution sources shaping stream macroinvertebrate communities. *Science of the Total Environment*, *587–588*, 1–10. https://doi.org/10.1016/j.scitotenv.2017.02.031

Blyth, K., & Rodda, J. C. (1973). A stream length study. *Water Resources Research*, *9*(5), 1454–1461. https://doi.org/10.1029/WR009i005p01454

Boodoo, K. S., Trauth, N., Schmidt, C., Schelker, J., & Battin, T. J. (2017). Gravel bars are sites of increased CO2 outgassing in stream corridors. *Scientific Reports*, *7*(1), 1–9. https://doi.org/10.1038/s41598-017-14439-0

Botter, G., Basso, S., Rodriguez-Iturbe, I., & Rinaldo, A. (2013). Resilience of river flow regimes. *PNAS*, *110*(32), 12925–12930. https://doi.org/10.1073/pnas.1311920110

Botter, G., & Durighetto, N. (2020). The stream length duration curve: A tool for characterizing the time variability of the flowing stream length. *Water Resources Research*, *56*(8). https://doi.org/10.1029/2020WR027282

Botter, G., Vingiani, F., Senatore, A., Jensen, C., Weiler, M., Mcguire, K., et al. (2021). Hierarchical climate-driven dynamics of the active channel length in temporary streams. *Scientific Reports*, *11*(1), 1–12. https://doi.org/10.1038/s41598-021-00922-2

Datry, T., Foulquier, A., Corti, R., Von Schiller, D., Tockner, K., Mendoza-Lera, C., et al. (2018). A global analysis of terrestrial plant litter dynamics in non-perennial waterways. *Nature Geoscience*, *11*(7), 497–503. https://doi.org/10.1038/s41561-018-0134-4

Datry, T., Larned, S. T., & Tockner, K. (2014). Intermittent rivers: A challenge for freshwater ecology. *BioScience*, *64*(3), 229–235. https://doi.org/10.1093/biosci/bit027

Day, D. G. (1978). Drainage density changes during rainfall. *Earth Surface Processes and Landforms*, *3*(3), 319–326. https://doi.org/10.1002/esp.3290030310

Dohman, J. M., Godsey, S. E., & Hale, R. L. (2021). Three-dimensional subsurface flow path controls on flow permanence. *Water Resources Research*, *57*(10). https://doi.org/10.1029/2020WR028270

Dunne, T., & Black, R. D. (1970). An experimental investigation of runoff production. *Water Resources Research*, *6*(2), 478–490. https://doi.org/10.1029/WR006i002p00478

Dupas, R., Abbott, B. W., Minaudo, C., & Fovet, O. (2019). Distribution of landscape units within catchments influences nutrient export dynamics. *Frontiers in Environmental Science*, *7*, 1–8. https://doi.org/10.3389/fenvs.2019.00043

Durighetto, N., Bertassello, L. E., & Botter, G. (2022). Eco-hydrological modelling of channel network dynamics—Part 1: Stochastic simulation of active stream expansion and retraction. *Royal Society Open Science*, *9*(11), 220944. https://doi.org/10.1098/rsos.220944

Durighetto, N., & Botter, G. (2021). Time-lapse visualization of spatial and temporal patterns of stream network dynamics. *Hydrological Processes*, *35*(2), 10–12. https://doi.org/10.1002/hyp.14053

Durighetto, N., & Botter, G. (2022). On the relation between active network length and catchment discharge. *Geophysical Research Letters*, *49*(14). https://doi.org/10.1029/2022GL099500

Durighetto, N., & Botter, G. (2023). Dataset: Extending active network vs catchment discharge relations to temporarily-dry outlets [dataset]. Research Data Unipd. https://doi.org/10.25430/researchdata.cab.unipd.it.00000912

Durighetto, N., Mariotto, V., Zanetti, F., Mcguire, K. J., Mendicino, G., Senatore, A., & Botter, G. (2022). Probabilistic description of streamflow and active length regimes in rivers. *Water Resources Research*, *58*(4), 1–24. https://doi.org/10.1029/2021WR031344

Durighetto, N., Vingiani, F., Bertassello, L. E., Camporese, M., & Botter, G. (2020). Intraseasonal drainage network dynamics in a headwater catchment of the Italian Alps. *Water Resources Research*, *56*(4). https://doi.org/10.1029/2019WR025563

Giezendanner, J., Benettin, P., Durighetto, N., Botter, G., & Rinaldo, A. (2021). A note on the role of seasonal expansions and contractions of the flowing fluvial network on metapopulation persistence. *Water Resources Research*, *57*(11), 1–18. https://doi.org/10.1029/2021wr029813

Godsey, S. E., & Kirchner, J. W. (2014). Dynamic, discontinuous stream networks: Hydrologically driven variations in active drainage density, flowing channels and stream order. *Hydrological Processes*, *28*(23), 5791–5803. https://doi.org/10.1002/hyp.10310

Goodrich, D., Kepner, W., Levick, L., & Wigington, P. (2018). Southwestern intermittent and ephemeral stream connectivity. *Journal of the American Water Resources Association*, *54*(2), 400–422. https://doi.org/10.1111/1752-1688.12636

Gregory, K. J., & Walling, D. E. (1968). The variation of drainage density within a catchment. *International Association of Scientific Hydrology Bulletin*, *13*(2), 61–68. https://doi.org/10.1080/02626666809493583

Jensen, C. K., McGuire, K. J., McLaughlin, D. L., & Scott, D. T. (2019). Quantifying spatiotemporal variation in headwater stream length using flow intermittency sensors. *Environmental Monitoring and Assessment*, *191*(4), 226. https://doi.org/10.1007/s10661-019-7373-8

Jensen, C. K., McGuire, K. J., & Prince, P. S. (2017). Headwater stream length dynamics across four physiographic provinces of the Appalachian Highlands. *Hydrological Processes*, *31*(19), 3350–3363. https://doi.org/10.1002/hyp.11259

Krabbenhoft, C. A., Allen, G. H., Lin, P., Godsey, S. E., Allen, D. C., Burrows, R. M., et al. (2022). Assessing placement bias of the global river gauge network. *Nature Sustainability*, *5*(7), 586–592. https://doi.org/10.1038/s41893-022-00873-0

Lapides, D. A., Leclerc, C. D., Moidu, H., Dralle, D. N., & Hahm, W. J. (2021). Variability of headwater stream network extents controlled by flow regime and network hydraulic scaling. *Hydrological Processes*, *35*(3). https://doi.org/10.1002/hyp.14079

Messager, M. L., Lehner, B., Cockburn, C., Lamouroux, N., Pella, H., Snelder, T., et al. (2021). Global prevalence of non-perennial rivers and streams. *Nature*, *594*(7863), 391–397. https://doi.org/10.1038/s41586-021-03565-5

Nikolaidis, N. P., Demetropoulou, L., Froebrich, J., Jacobs, C., Gallart, F., Prat, N., et al. (2013). Towards sustainable management of Mediterranean river basins: Policy recommendations on management aspects of temporary streams. *Water Policy*, *15*(5), 830–849. https://doi.org/10.2166/wp.2013.158

Perez, A. B. A., Innocente dos Santos, C., Sá, J. H. M., Arienti, P. F., & Chaffe, P. L. B. (2020). Connectivity of ephemeral and intermittent streams in a subtropical Atlantic forest headwater catchment. *Water*, *12*(6), 1526. https://doi.org/10.3390/w12061526

Prancevic, J. P., & Kirchner, J. W. (2019). Topographic controls on the extension and retraction of flowing streams. *Geophysical Research Letters*, *46*(4), 2084–2092. https://doi.org/10.1029/2018GL081799

Reyjol, Y., Argillier, C., Bonne, W., Borja, A., Buijse, A. D., Cardoso, A. C., et al. (2014). Assessing the ecological status in the context of the European Water Framework Directive: Where do we go now? *Science of the Total Environment*, *497–498*, 332–344. https://doi.org/10.1016/j.scitotenv.2014.07.119

Roberts, M. C., & Archibold, O. W. (1978). Variation of drainage density in a small British Columbia watershed. *Journal of the American Water Resources Association*, *14*(2), 470–476. https://doi.org/10.1111/j.1752-1688.1978.tb02183.x

Rodriguez-Iturbe, I., Rinaldo, A., & Levy, O. (1998). Fractal River basins: Chance and self-organization. *Physics Today*, *51*(7), 70–71. https://doi.org/10.1063/1.882305

Senatore, A., Micieli, M., Liotti, A., Durighetto, N., Botter, G., Mendicino, G., & Botter, G. (2020). Monitoring and modeling drainage network contraction and dry down in mediterranean headwater catchments. *Water Resources Research*, *57*(6). https://doi.org/10.1029/2020WR028741

Seybold, E. C., Anna, B., Jones, C. N., Burgin, A. J., Zipper, S., Godsey, S. E., et al. (2023). How low can you go? Widespread challenges in measuring low stream discharge and a path forward. *Limnology and Oceanograpy Letters*, *8*(6), 804–811. https://doi.org/10.1002/lol2.10356

Shaw, S. B., Bonville, D. B., & Chandler, D. G. (2017). Combining observations of channel network contraction and spatial discharge variation to inform spatial controls on baseflow in Birch Creek, Catskill Mountains, USA. *Journal of Hydrology: Regional Studies*, *12*, 1–12. https://doi.org/10.1016/j.ejrh.2017.03.003

Skoulikidis, N. T., Sabater, S., Datry, T., Morais, M. M., Buffagni, A., Dörflinger, G., et al. (2017). Non-perennial Mediterranean rivers in Europe: Status, pressures, and challenges for research and management. *Science of the Total Environment*, *577*, 1–18. https://doi.org/10.1016/j.scitotenv.2016.10.147

Tsegaw, A. T., Skaugen, T., Alfredsen, K., & Muthanna, T. M. (2020). A dynamic river network method for the prediction of floods using a parsimonious rainfall-runoff model. *Hydrology Research*, *51*(2), 146–168. https://doi.org/10.2166/nh.2019.003

Vander Vorste, R., Sarremejane, R., Datry, T., Vorste, R. V., Sarremejane, R., & Datry, T. (2020). *Intermittent rivers and ephemeral streams: A unique biome with important contributions to biodiversity and ecosystem services* (Vol. 4). Elsevier Inc. https://doi.org/10.1016/b978-0-12-409548-9.12054-8

von Schiller, D., Marcé, R., Obrador, B., Gómez-Gener, L., Casas-Ruiz, J. P., Acuña, V., & Koschorreck, M. (2014). Carbon dioxide emissions from dry watercourses. *Inland Waters*, *4*(4), 377–382. https://doi.org/10.5268/IW-4.4.746

Ward, A. S., Schmadel, N. M., & Wondzell, S. M. (2018). Simulation of dynamic expansion, contraction, and connectivity in a mountain stream network. *Advances in Water Resources*, *114*, 64–82. https://doi.org/10.1016/j.advwatres.2018.01.018

Zanetti, F., Durighetto, N., Vingiani, F., & Botter, G. (2021). Analysing river network dynamics and active length – Discharge relationship using water presence sensors. *Hydrology and Earth System Sciences Discussions*, 1–27. https://doi.org/10.5194/hess-2021-103

Zimmer, M. A., & McGlynn, B. L. (2017). Ephemeral and intermittent runoff generation processes in a low relief, highly weathered catchment. *Water Resources Research*, *53*(8), 7055–7077. https://doi.org/10.1002/2016WR019742

Zimmermann, B., Zimmermann, A., Turner, B. L., Francke, T., & Elsenbeer, H. (2014). Connectivity of overland flow by drainage network expansion in a rain forest catchment. *Water Resources Research*, *50*(2), 1457–1473. https://doi.org/10.1002/2012WR012660